The Creation of PEGylated pH-Triggered Self-Assembling Peptide Amphiphiles for Long-Circulating Cancer Targeting MRI Contrast Agents

Undergraduate Honors Research Thesis

Presented in Partial Fulfillment of the Requirements for graduation "with Honors Research Distinction in Chemistry" in the Arts and Sciences of The Ohio State University

By:

Emily Ann Hawley Paradis

The Ohio State University

April 2017

Honors Defense Committee:

Professor Joshua Goldberger (Project Advisor)

Professor Jonathan Parquette

Table of Contents

Acknowledgements:

I would like to thank the graduate students that mentored me during my undergraduate career, which includes Ashley J. Wallace and Christian Buettner. I want to thank Dr. Elizabeth Alexander for her training and continued patience on the Electrospray Ionization Mass Spectrometer. Dr. Marina Bakhtina also has my gratitude for training me to use the Jasco Circular Dichroism Spectrometer. I would especially like to thank Dr. Josh Goldberger for his influence and mentorship during my research experience.

Vita:

Education:

The Ohio State University, Columbus OH

Bachelor of Science, Biochemistry, 2017

Minor in Psychology

Magna Cum Laude

Hilliard Darby High School, Hilliard, OH

Honors Diploma, 2013

Abstract:

To date there is no Magnetic Resonance Imaging (MRI) contrast agent that selectively targets cancer, despite it being the highest resolution diagnostic technique. The challenge lies with designing a biocompatible FDA- approvable contrast agent that can locally accumulate only in the extracellular environment of tumor tissue at a 10 μM concentration. To accumulate an imaging agent selectively in the tumor tissue we have established a new class of self-assembling vehicles that circulate through the body as 10 nm spherical micelles and transition into slowly diffusing μm-long fibers upon entering the acidic extracellular vasculature of tumor tissue. However, to maximize accumulation, it is essential to maximize the amount of time that these vehicles circulate through the blood stream before they are cleared by the immune system. The addition of a polyethylene glycol (PEG) shell to circulating vehicles is a well-established method for minimizing an immune response, and allowing long circulation. However, incorporating this PEG shell onto these transitioning peptide amphiphile (PA) vehicles impacts their self-assembly behavior. Here, we have established the influence of PEG on the transitioning properties of these PAs through the characterization of the pH – concentration phase diagrams of different mixtures of 2000 kDa PEGylated and unPEGylated PAs. We show that PEG termination disrupts self-assembly, resulting in an increased critical micelle concentration and a more acidic nanofiber to micelle transition. PAs that have greater propensity to form nanofibers need more relative amounts of PEGylated PAs to maintain a transition at a uniform pH. In conclusion, we show that it is indeed possible to create a PEGylated vehicle that transitions in a serum environment at a pH of 7, which will enable the creation of a long-circulating transitioning MRI contrast agent.

Chapter 1: Introduction

Cancer accounts for approximately 1 of every 4 deaths in the United States. According to the American Cancer Society, in 2017, 1,688,780 people will be diagnosed with cancer and 600,920 Americans will die of cancer[1]. The key to decreasing cancer mortality, according to reports by the American Cancer Society is to develop better methods for early detection[2]. As an example, the 5-year survival rate for patients having localized breast cancer is 98.6%, which is reduced to 23.3% after it metastasizes[3]. Currently, most cancer is detected at later stages when symptoms are presented[2]. Developing an imaging modality that can selectively detect cancerous tissue at early stages with small (< 1 cm) tumor sizes will enable earlier treatments, and likely decreased mortality. Compared to all the imaging modalities that exist (Near Infrared Imaging, MRI, and Positron Emission Tomography), MRI gives the highest spatial resolution (< 1 mm) and is noninvasive[4]. However, the challenge with MRI lies with the fact that a contrast agent that selectively accumulates in tumor tissue across a broad range of cancer types at an imaging concentration of >10 μM is needed[5,6]. No such MRI agent currently exists.

This research aims to develop such an imaging agent. We seek to take advantage of the hallmarks common to all cancer types that are distinct from healthy tissue. One such hallmark of cancer is the upregulation of anaerobic glycolysis[7]. This results in an acidic microenvironment around the tumor cells due to the production of lactic acid, which is excreted from cancer cells[7]. Typically the extracellular pH (pHe) for tumor tissue can range from 6.4-7.4, depending on the rate of growth[7,8]. A second hallmark is the leakiness of tumor vasculature, which can increase the rate of drug delivery to the tumor. The cells of the endothelial layer of the vessels are irregular and disorganized and

thus permit some leaking of vessel components through the walls. The leaked vessel components are then somewhat retained by the tumor due to poor lymphatic drainage. These two characteristics are known as the Enhanced Permeability and Retention (or EPR) effects[9,10,11].

Research in the Goldberger lab has previously taken advantage of these hallmarks to create nanovehicles that transition in response to the acidic microenvironment and accumulate at the tumor site (Figure 1)[12]. The overall ideal is to develop a self-assembling vehicle that circulates through the bloodstream as either a spherical micelle or small molecule at the normal blood pH of 7.4. Once it diffuses into the acidic tumor vasculature, it self-assembles into a much larger, more slowly-diffusing nanofiber. Such a mechanism should maximize the accumulation of vehicles in the tumor tissue, since diffusion is the main mechanism for which vehicles and enter and leave the tumor microenvironment. The challenge lies with creating vehicle that can undergo such a transition in vivo.

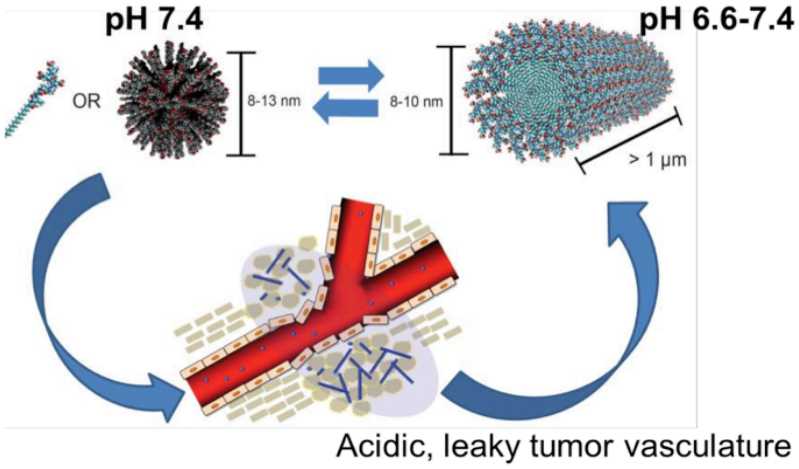

Figure 1: An overview of the PA's morphological transition when interacting with the acidic microenvironment of a tumor. In this design, single molecules or spherical micelles circulate through the blood stream at a pH of 7.4, then diffuse into the acidic leaky vasculature of tumor tissue, allowing for a self-assembly transition into a much larger nanofiber morphology.

The Goldberger lab has established PA nanovehicles that can undergo such a pH-dependent transition in pure blood serum[12]. PAs are a class of self-assembling molecules comprised from biocompatible building blocks (peptides and lipids) that can be thought of as peptide surfactants. These molecules typically contain a hydrophobic region, a B-sheet forming region, a charged region, and a region that chelated to an MRI contrast agent (Figure 2)[12,13,14,15]. Typically, 1,4,7-tris(carboxymethylaza)cyclododecane-10-azaacetylamide (DO3A) moiety is attached to at terminal lysine, which chelates the Gd^{3+} imaging agent. The surfactant-like nature of these molecules enables them to self-assemble into spherical micelles, 1D nanofibers upon the presence of the β -sheet depending on the pH and concentration, and solution environment[16,17]. When a micelle forms, the hydrophobic tails arrange in the center of the micelle, allowing the charged regions to interact with the aqueous environment. A nanofiber forms when the attraction between amino acids in the β-sheet region overcome the electrostatic repulsion induced by the charged amino acid residues, enabling the formation of β -sheets along the length of the fiber. These β-sheets consist of hydrogen bonding interactions between neighboring molecules.

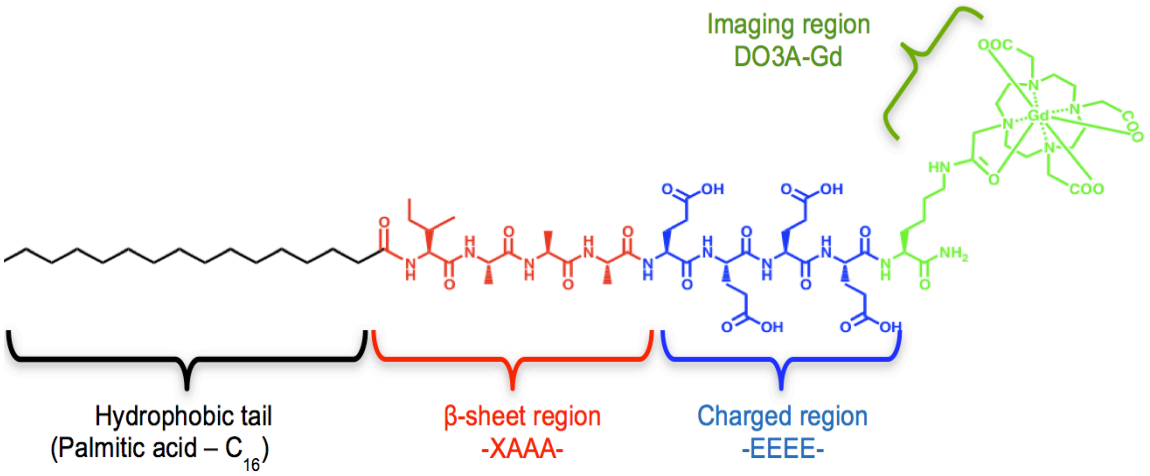

Figure 2: The structure of a peptide amphiphile (PA). The PA has a hydrophobic tale, a B sheet region, which promotes the formation of nanofibers, a charged region, which promotes the formation of micelles, and an imaging region.

Initial *in vivo* biodistribution tests in tumor animals show appreciable accumulation in the tumor tissue, as well as the liver, lungs, and spleen, which is indicative of an immune system response[18]. The detection by the mononuclear phagocyte system (MPS) are reasons for the clearance of the PAs by these organs[18]. One standard method to minimize vehicular uptake by the immune system is to add a polyethylene glycol (PEG) moiety to its outer surface. PEG is an FDA-approved polymer that commonly coats biomaterials by preventing opsonization and removal from the immune system[19,20].

The goal of this thesis, is to understand how the addition of different relevant amounts of a 2000 Da PEG (PEG2k) moiety to the outer terminus affects the self-assembly properties of these PAs, as well as design a formulation that can transition in a simulated blood serum environment at a pH of 6.6-7.0. To accomplish this we synthesized and characterized the self-assembly properties of two different PAs that have varying amino acids in the B-sheet forming region (Table 1, Figs 3-5). Specifically, we

have developed two PAs that feature Valine (V) or Isoleucine (I) in the β -sheet forming region, (palmitoyl-VAAAEEEEK(DO3A:Gd)-NH_2, and palmitoyl-IAAAEEEEK(DO3A:Gd)-NH_2, as PA1 and PA2, respectively). Then mixtures of non-PEGylated PA with varying percentages of palmitoyl-MAAAEEEEK(PEG2k)-NH_2 (PA3PEG) were prepared and the changes in the pH- and concentration-dependent self-assembly phase diagram were characterized. Overall, we showed that the addition of PA3PEG to the mixture disrupts micelle and nanofiber formation, leading to increases in the critical micelle concentration and more acidic nanofiber to micelle transitions. PA2, which features a greater propensity to form nanofibers than PA1, needs a greater concentration of PA3PEG to induce a micelle to nanofiber transition at pH of 7[21]. In conclusion, we show that it is indeed possible to create a PEGylated vehicle that transitions in a simulated serum environment at a pH of 7. This work will enable future biodistribution studies evaluating the accumulation of these vehicles in a simulated serum environment.

Table 1: A summary of the sequence of the PAs synthesized in this work.

Molecule	***Sequence***
PA1	palmitoyl-VAAAEEEEK(DO3A:Gd)-NH_2
PA2	palmitoyl-IAAAEEEEK(DO3A:Gd)-NH_2
PA3PEG	palmitoyl-MAAAEEEEK(PEG2k)-NH_2

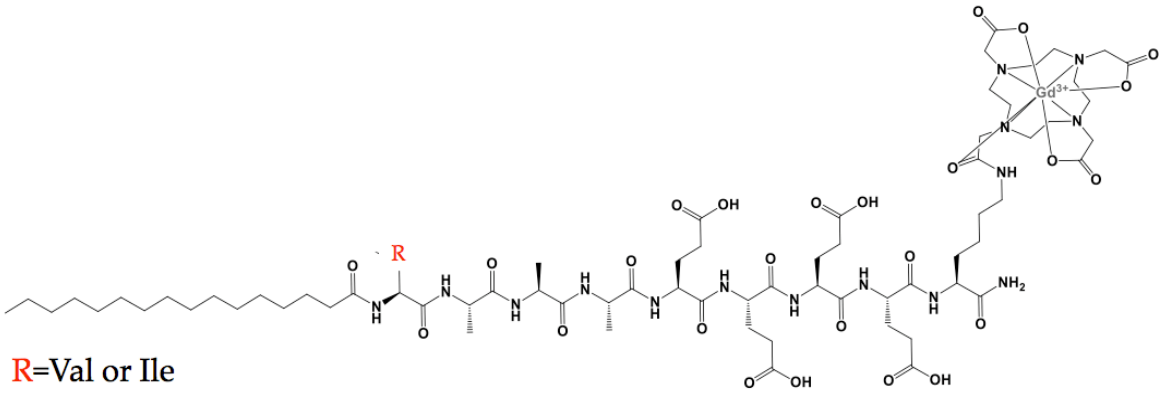

Figure 3: *Structure of PA1 or PA2*

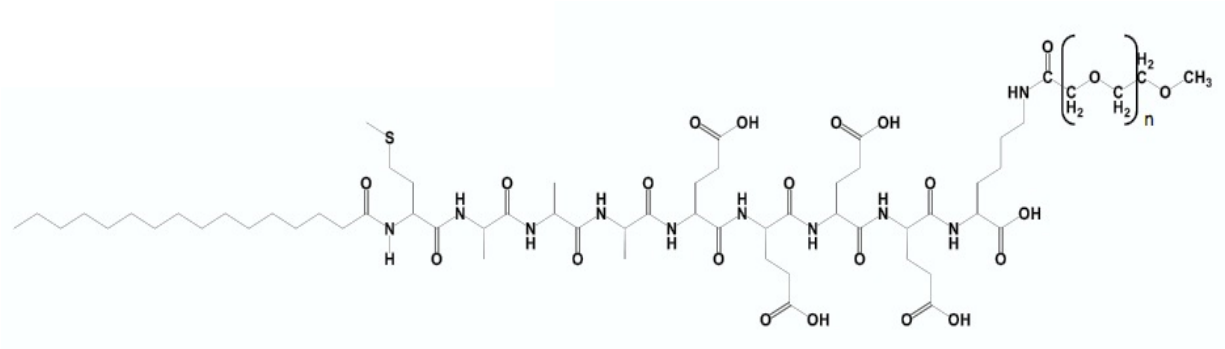

Figure 4: Structure of PA3PEG

Chapter 2: PA Synthesis

All PAs were synthesized using traditional solid-phase peptide synthesis. Amino acids were coupled using Fluorenylmethoxycarbonyl (FMOC) chemistry from the C-terminus to the N-terminus. Additionally, the PAs were synthesized on a 0.5-0.75 mmol scale using a Sieber amide resin. The resin was added to a shaker vessel with dichloromethane (DCM) and shaken. After 30 minutes the DCM was removed and dimethyl formamide (DMF) was shaken with the resin for 30 minutes. The FMOC using 20% piperidine in DMF, which was shaken for 20 minutes twice. Afterwards, a Kaiser test was run to confirm that the deprotection was successful. If the test turns blue, the amine is primary. Then 4 equivalents of the amino acid were mixed with either 4 equivalents of O- Benzotriazole N,N,N',N'-tetramethyluronium hexafluoro-phosphate (HBTU), or 2-(7-Aza- 1H-benzotriazole-1-yl)-1,1,3,3 tetramethyluronium hexafluorophosphate (HATU) as coupling agents, along with 6 equivalents of N,N-diisopropyl-ethylamine (DIPEA), and 2 drops of Triton X-100 surfactant in approximately 10mL of DMF. The first amino acid coupled on the resin was lysine, which featured an ε-NH-methyltrityl (MTT) protecting group. This mixture was shaken for at least 2 hours. Afterwards, it was rinsed with DCM and DMF. A Kaiser test was run again to confirm the coupling of the amino acid. If the test stays yellow, it is confirmation of a successful coupling yielding no free amines. This cycle is repeated to couple the subsequent amino acids as well as the palmitic acid chain.

The next steps in PA synthesis involve cleaving from the resin and coupling either PEG2k or DO3A to the terminal lysine residue. The PAs were cleaved from the resin 1% Trifluoroacetic acid (TFA), 1% Triisopropyl silane (TIS), 2% Anisole and 96% DCM.

This cleavage solution both cleaves the PA from the resin as well as deprotects the MTT protecting group attached to the terminal lysine. After precipitating the PA out of solution with cold distilled water it was dried and solubilized with 15mL of pyridine through heating (60 ºC to couple either DO3A or PEG2k to the terminal lysine. To couple with DO3A, the solubilized PA was mixed at room temperature with 2 eq. HATU, 2 eq. DO3A, and 4.4 eq. DIPEA for 18-24 hours. A second addition of 2 eq. HATU and 4.4 eq. DIPEA were added to the mixture for 2 more hours. The PA was then precipitated out of solution with cold distilled water and dried. The solid was mixed with 95% TFA, 1% TIS, 2% Anisole, 2% water to remove the protecting tert-butyl groups. The PA was then precipitated out with cold diethyl ether and dried.

The crude PA was purified with High Performance Liquid Chromatography (HPLC) using a preparative scale Shimadzu duel pump system and an Agilent PLRP-S polymer column. The PA was solubilized in 9 mL of distilled water and 1 mL of acetonitrile, basified with a couple drops of NH_4OH. The solution was filtered through a 0.45 μm PVDF filter before injection. A gradient of acetonitrile with 0.1% NH_4OH was increased from 10% to 100% over the HPLC column to elute out the PA. To identify which HPLC fractions contained the PA they were analyzed with ESI-TOF Mass Spectrometry. A couple drops of the fraction solution were serially diluted in 5 mL of methanol (MeOH). About 200 μL of the most dilute sample was injected into a Bruker Daltonics MicroTOF Mass Spectrometer for mass analysis.

Fractions with significant signals corresponding to the PA mass were analyzed with a Shimadzu analytical HPLC dual pump system. The purified PA was solubilized in distilled water and a couple drops of NH_4OH was filtered with a 0.2 μm filter and

injected into the analytical HPLC. A gradient of acetonitrile from 10% to 100% with 0.1% NH_4OH was applied over the column to elute out the PA to test the fractions for purity. Fractions with at least 95% purity were combined, rotovapped and lyophilized to dry powder.

Gd^{3+} was then chelated to the pure DO3A terminated PAs. ~10-20 mg of pure PA was dissolved in ~ 5 mL distilled water and 2 eq. of 0.01 M $GdCl_3$ in 0.01 M HCl. The solution pH was adjusted to ~5.0 with diluted NaOH. The solution was stirred for an hour at 60ºC in an oil bath, readjusted to a pH ~5.0, and stirred for 12-18 hours in the heated oil bath. The pH was then adjusted to ~10 to precipitate the excess Gd^{3+}. The solution was then passed through a 0.45 μm PVDF filter. The solution was then dialyzed to remove the excess salts using a Spectra/Por® Biotech Cellulose Ester dialysis membrane (molecular weight cut off: 500 g/mol). The dialysis water was changed every 2 hours over the course of 12 hours. The dialyzed solution was then lyophilized to form dry powder.

Mass Spec and Analytical HPLC were used to purify the PA samples. Figure 5, Figure 6, and Figure 7 show the MS-ESI of PA1, PA2, and PA3PEG respectively. The largest peak seen corresponds to the mass of the synthesized PA. Figure 8, Figure 9, and Figure 10 show the analytical HPLC to confirm purity of the PA samples.

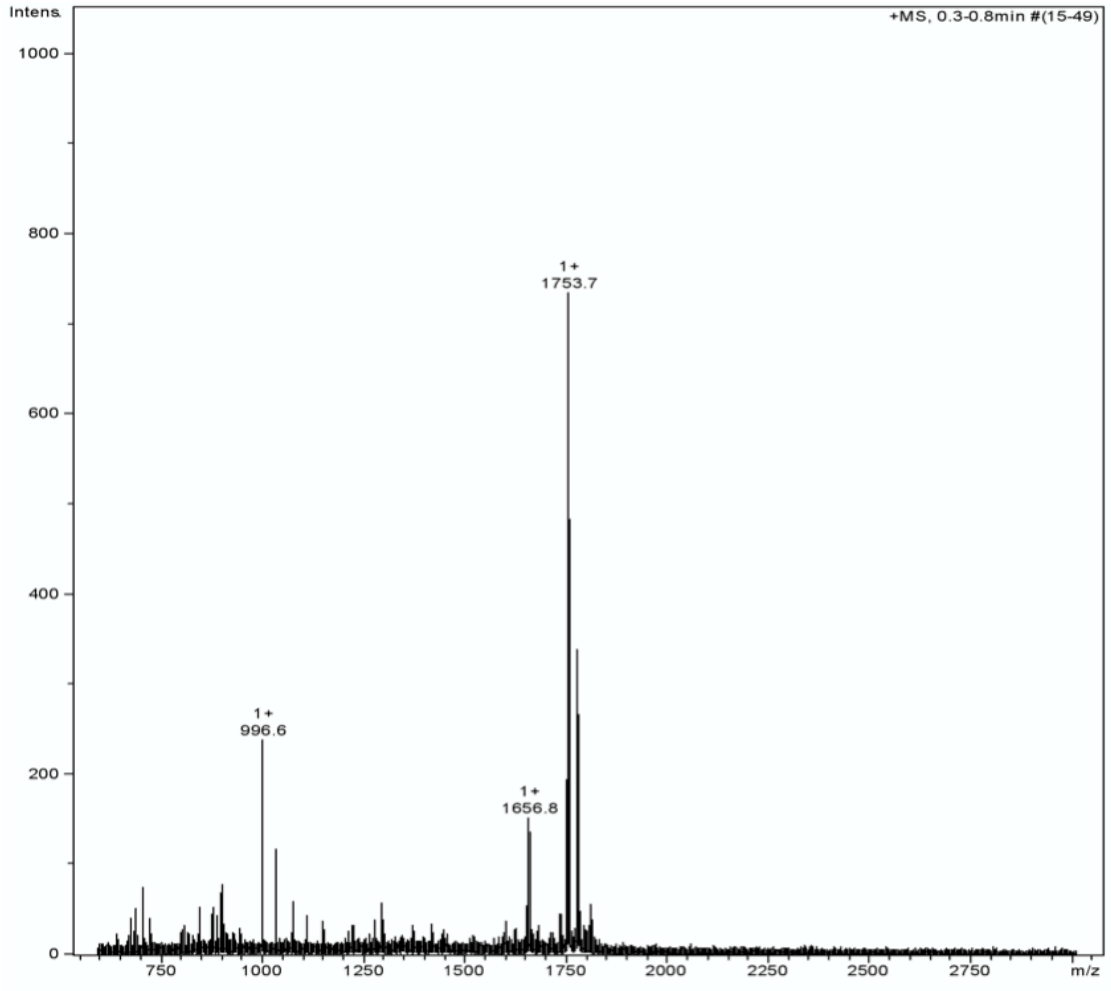

Figure 5: Mass Spectrometry of PA1 M/Z=1752.

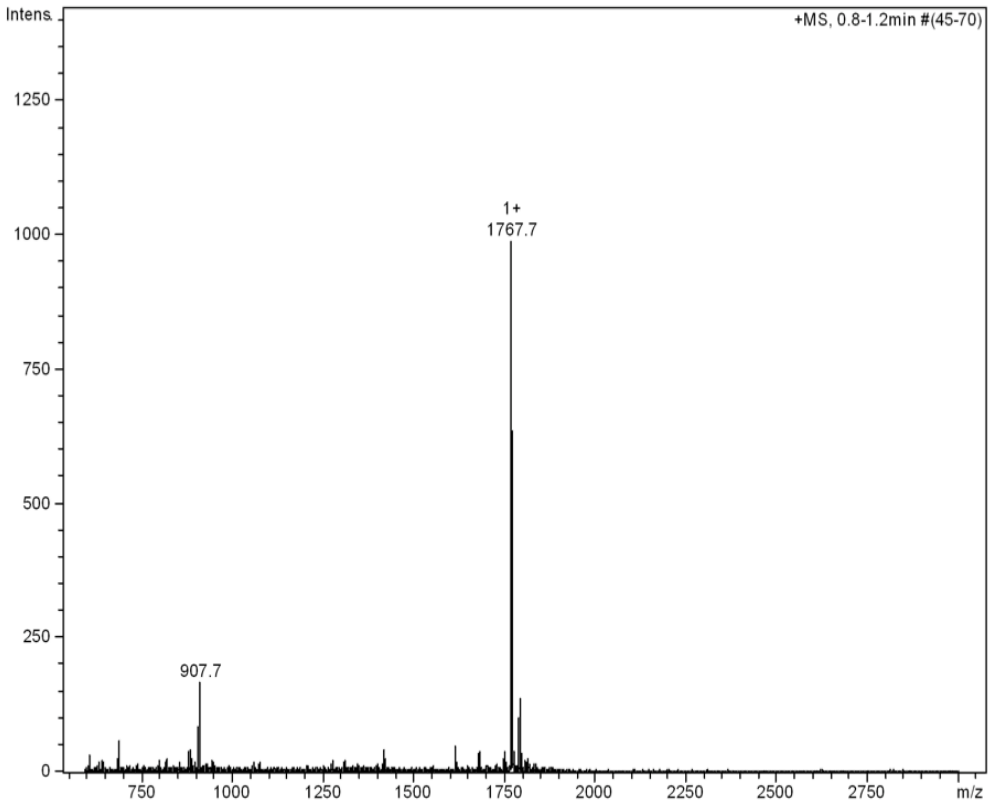

Figure 6: Mass Spec of PA2 M/Z=1766

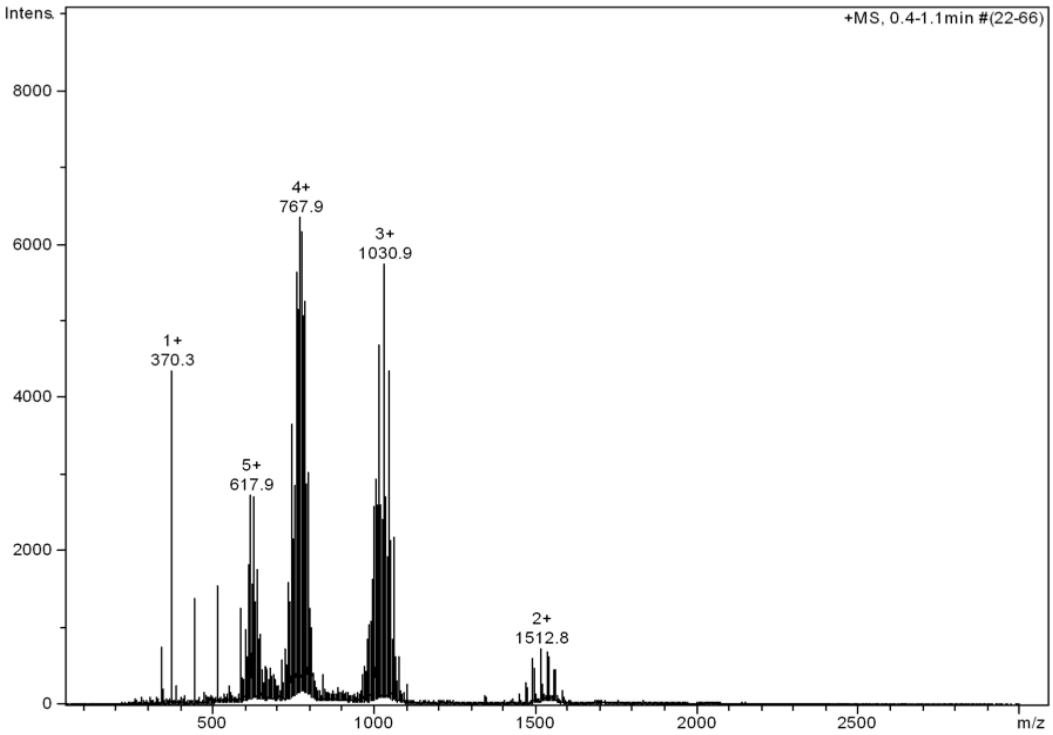

Figure 7: Mass Spec of PA3PEG M/z~3020

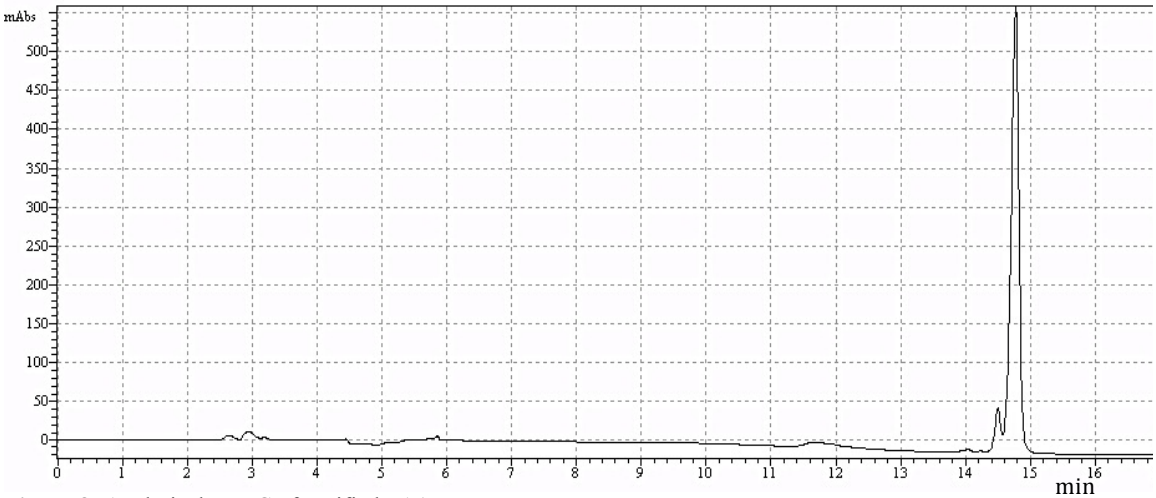

Figure 8: Analytical HPLC of purified PA1

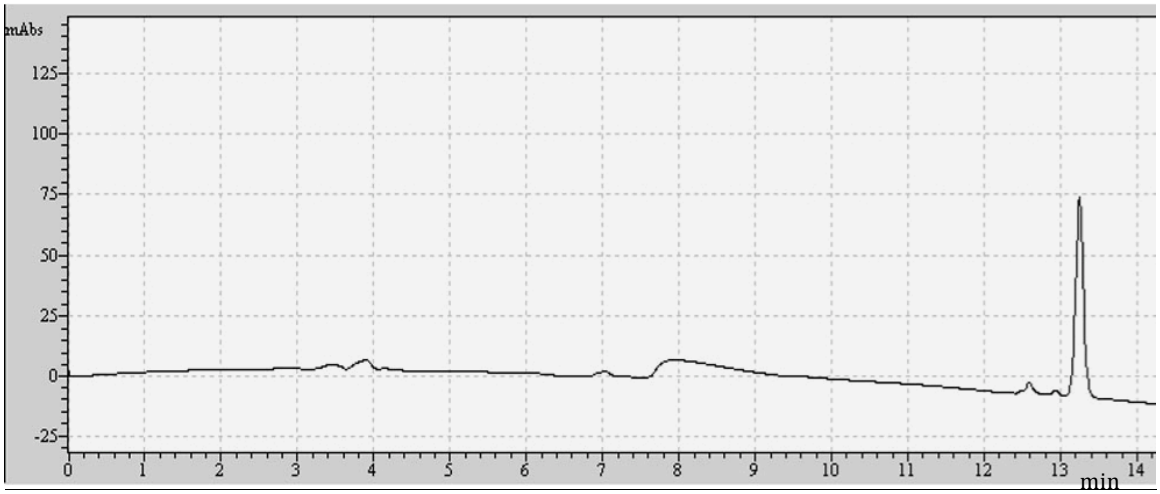

Figure 9: Analytical HPLC of PA2

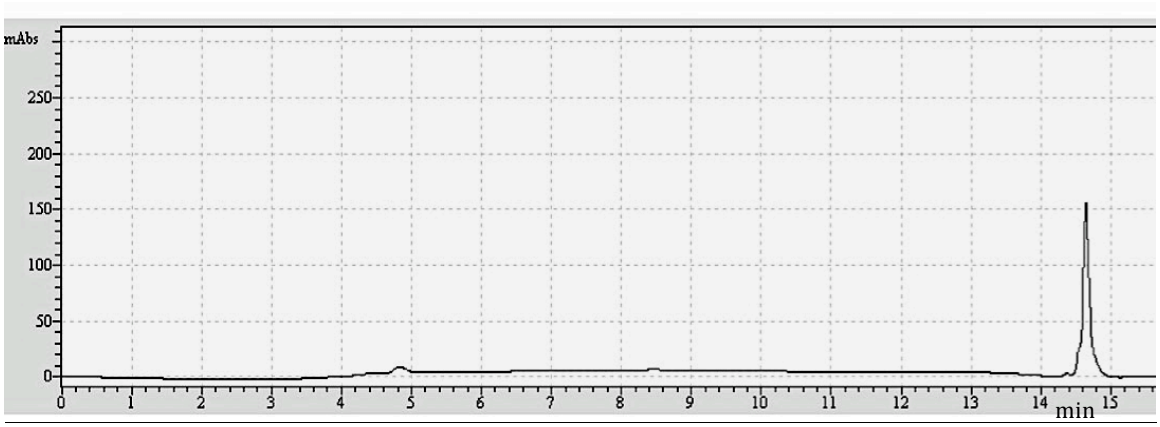

Figure 10: Analytical HPLC of PA3PEG

Chapter 3: Self-Assembly Behavior

Our next goal was to understand the influence of adding different concentrations of PA3PEG on the self-assembly behavior of PA1 and PA2. The pH and concentration dependent self-assembly behavior was characterized for all PAs in an artificial serum solution that mimics the complex environment of pure blood serum. The Goldberger lab previously established that an artificial serum solution containing 150 mM NaCl, 2.2 mM $CaCl_2$, and 1.8 mM 20 kDa PEG effective simulates the ionic strength and molecular crowding environment of pure blood serum, showing very similar pH-dependent self-assembly behavior.[22] The lack of any proteins in this media allows the use of Circular Dichroism (CD) and critical micelle concentration measurements using the pyrene 1:3 method to characterize the self-assembled morphology of the PA.

The PAs were prepared for Circular Dichroism (CD) measurements on the Jasco-815 Circular Dichroism spectrometer. PAs were prepared in this artificial serum medium with varying percentages of PA3PEG. The solution was basified to a pH >9 and stirred at 90 ^{o}C for 30 minutes. After the solution was cooled, the pH was readjusted. Measurements were conducted in 0.5-1 cm path length quartz cuvettes. The pH of the solution is lowered in increments to see the pH range for which the PAs shift from random coil to a nanofiber assembly. Data was collected from wavelength 250-190 nm. A β-sheet secondary structure is defined as one with a local minimum in the ellipiticity around 218 nm, and an increasing ellipticity at lower wavelengths. A random coil secondary structure has a The crossing of the x-axis around 218 nm indicates a shift to a nanofiber assembly[22]. A cuvette with distilled water was run to serve as a baseline to be subtracted from the other measurements.

The Goldberger lab has previously analyzed secondary structure transitions of 10 μM of PA2 and PA1 in a salt solution (150 mM NaCl, 2.2 mM $CaCl_2$).[23] The increased β-sheet propensity of the isoleucine residue in PA causes it transition from random coil to β-sheet morphologies at a higher pH (pH=5.65) than the transition for the valine-containing PA1 (pH = 5.27). We then collected the CD spectra of both PAs in the artificial serum media comprised of 150 mM NaCl, 2.2 mM $CaCl_2$ and 1.8 mM 20 kDa PEG. For both PA1 and PA2, only beta-sheet morphologies were observed from 10 μM-500 μM at pH values ranging from 5-10, indicating no self-assembly transition occurs.

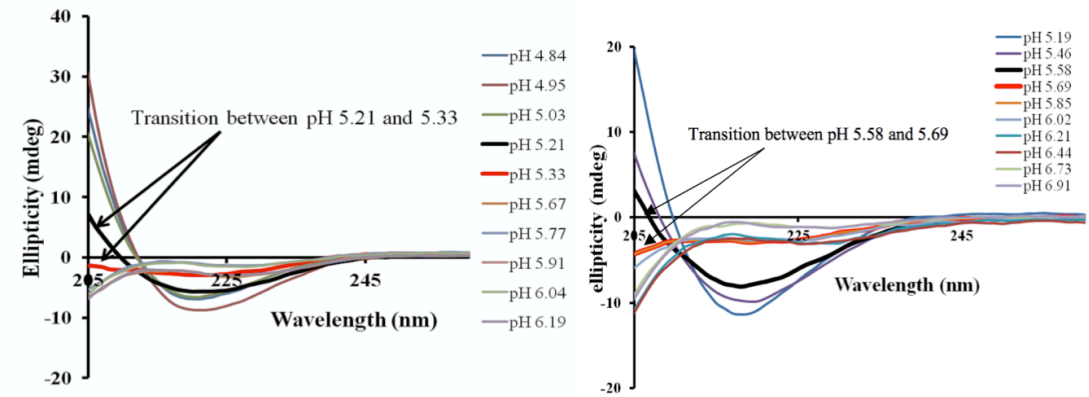

Figure 11: PA1 (left) and PA2 (right) CD at different pH values at 10 μM, 150 mM NaCl, 2.2 mM $CaCl_2$. Figure taken with permission from Ref 23.[23]

The Critical Aggregation Concentration (CAC) is the lowest concentration at a given pH when the PAs will self-assemble into structures. The PAs were made into solutions with varying percentages of PA3PEG with 150 mM NaCl and 2.2 mM $CaCl_2$ with 1.8 mM PEG. The PA solutions were made between 100 nM and 700 μM with serial dilutions. Each concentration sample also had 6 μM of pyrene and HCl or NaOH to adjust the pH. The solution is then pipetted into 96-well plates and the fluorescence is

monitored with a hybrid reader fluorometer. When reaching higher concentrations, the PAs self assemble, which encapsulates the pyrene in solution. This is seen as a change in slope of I_{376}/I_{392} when excited at 335 nm, which is what we used to determine the CAC.

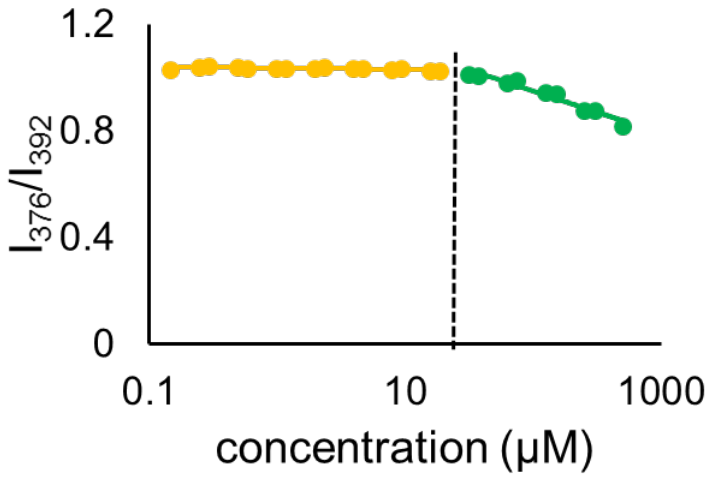

Figure 12:PA1 with 3.5% PA3PEG at pH7 in artificial serum. CAC value determined to be 30.5 μM.

Transmission Electron Microscopy (TEM) images were collected to visualize the PAs self-assembly at different pH values and concentrations. They were obtained with a FEI Tecnai G2 Bio TWIN TEM system. The samples were prepared for TEM in 150 mM NaCl, 2.2 mM $CaCl_2$, at 100 μM PA in 1.5% artificial serum. The samples without serum were heated and all samples had pH adjustments using HCl or NaOH. The samples were then carefully pipetted on Carbon Formvar grid, allowed to sit for a minute, and then the excess liquid was carefully removed with filter paper. The samples on the grid were stained with 1 wt% uranyl acetate.

CD and CAC data compiled generated phase diagrams, which are able to show at what pH and concentrations the PA mixtures will self assemble. The CMC's on the diagrams are represented by the horizontal lines at fixed pH values. They indicate the threshold concentration at which the PAs self assemble into either micelles or nanofibers.

The CD data on the graph is seen as the vertical/diagonal lines at fixed concentrations. They indicate the pH at which a micelle will transition to a nanofiber.

Figure 13 shows the phase diagram of $C_{16}VA_3E_4K$(DO3A:Gd)-NH_2 with 3.5%, 4%, and 5% $C_{16}MA_3E_3K$(PEG2k)-NH_2 prepared in artificial serum. The CAC values increase as PA3PEG % increases. This shows that a higher PA3PEG% in solution disrupts the self-assembly of the PAs. The solution needs to have a higher PA concentration for to initiate self-assembly at the same pH if the PA3PEG concentration is higher. Figure 13 also shows the pH of transition from micelle assembly to nanofiber assembly. Here, the graph shows that the 4% PA3PEG mixture has a higher pH of transition than the 3.5% PA3PEG mixture. This means it takes a lower pH for the 3.5% PA3PEG mixture to transition than the 4% PA3PEG mixture. This is true too for the 4% PA3PEG mixture in relation to the 5% PA3PEG mixture.

Table 2: CAC data from varying PA3PEG concentrations with PA1 in artificial serum.

pH	5%	4%	3.5%
9	88.8μM	47.1μM	16.2μM
7	100.8μM	73.0μM	30.5μM
5.5	114.5μM	80.5μM	47.4μM

Table 3: Nanofiber-micelle transition pH determined from CD data at overall PA concentrations (of 100 µM, 300 µM, and 500 µM) in artificial serum, different formulations varying PA3PEG concentrations with PA1 in artificial serum.

%PA3PEG In PA1	**500µM**	**300µM**	**100uM**
5%	7.79	6.45	6.34
4%	7.87	6.67	6.56
3.5%	7.89	6.63	6.65

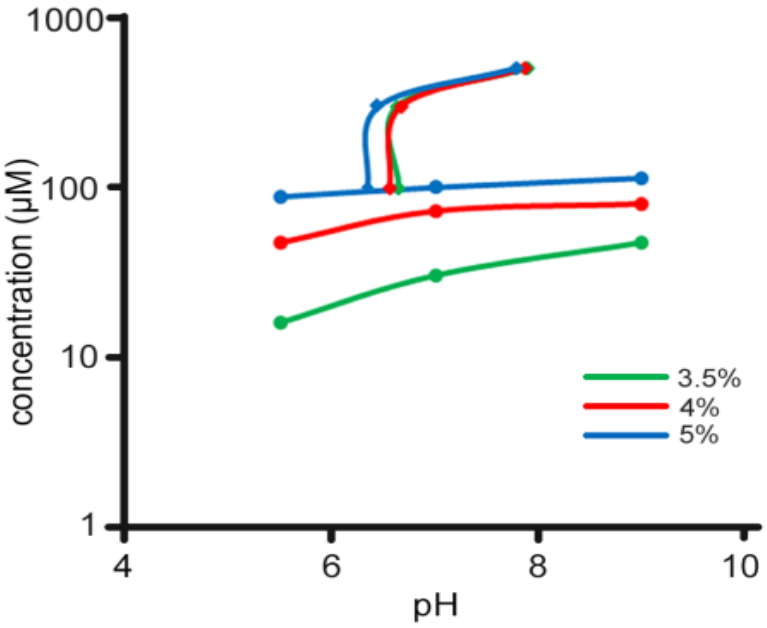

Figure 13: Phase diagram complied from CD (diamonds) and CAC (spheres) data of varying concentrations of PA3PEG in relation to PA1 in artificial serum.

TEM images of $C_{16}VA_3E_4KDO3A$:Gd were taken in various acidic and concentrated solutions that caused the PAs to assemble as nanofibers as predicted by the CD and CMC. The images confirmed the presence of fibers in the PA3PEG mixture

under acidic (pH=5.5) and concentrated (300 μM) conditions. The average diameter of the fibers was about 12 nm, which is in line with expected nanofiber diameters.

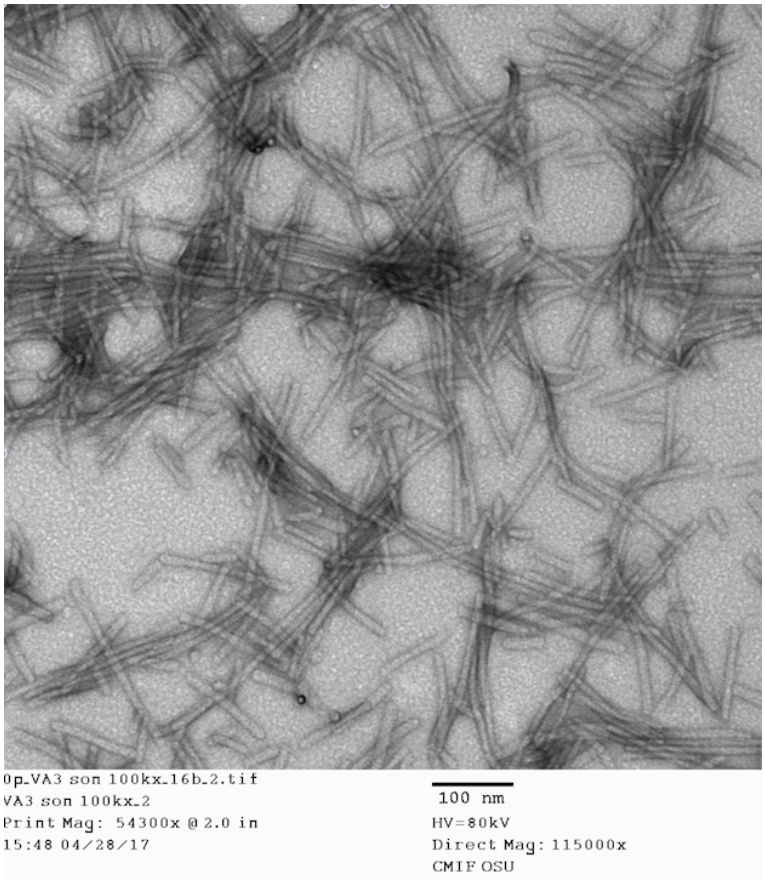

Figure 14: TEM images with a 100nm scale bar confirming nanofiber morphology of PA1 with 3.5% PA3PEG under acidic and high concentration conditions**. Fibers are measured to be 12nm in diameter.**

Figure 15 shows the phase diagram of $C_{16}IA_3E_4K$(DO3A:Gd)-NH_2 with 11%, and 13% $C_{16}MA_3E_3K$(PEG2k)-NH_2 prepared in artificial serum. The CAC values increase as PA3PEG % increases. This shows that a higher PA3PEG% in solution disrupts the self-assembly of the PAs. The solution needs to have a higher PA concentration for to initiate self-assembly at the same pH if the PA3PEG concentration is higher. Figure 15 also shows the pH of transition from micelle assembly to nanofiber assembly. Here, the graph shows that the 11% PA3PEG mixture has a higher pH of transition than the 13%

PA3PEG mixture. This means it takes a lower pH for the 11% PA3PEG mixture to transition than the 13% PA3PEG mixture.

Table 4: Random coil –self-assembled transition concentration determined from CAC data at pH's of 5.5,7, and 9 in artificial serum at varying PA3PEG concentrations with PA2.

pH	13%	11%
9	117.6 μM	35 μM
7	112.3 μM	52.3 μM
5.5	107.7 μM	16.3 μM

Table 5. Nanofiber-micelle transition pH determined from CD data at overall PA concentrations (of 100 μM, 300 μM, and 500 μM) in artificial serum, different formulations varying PA3PEG concentrations with PA2.

	500μM	300μM	100μM
13%	7.68	6.98	6.58
11%	8.04	7.54	6.72

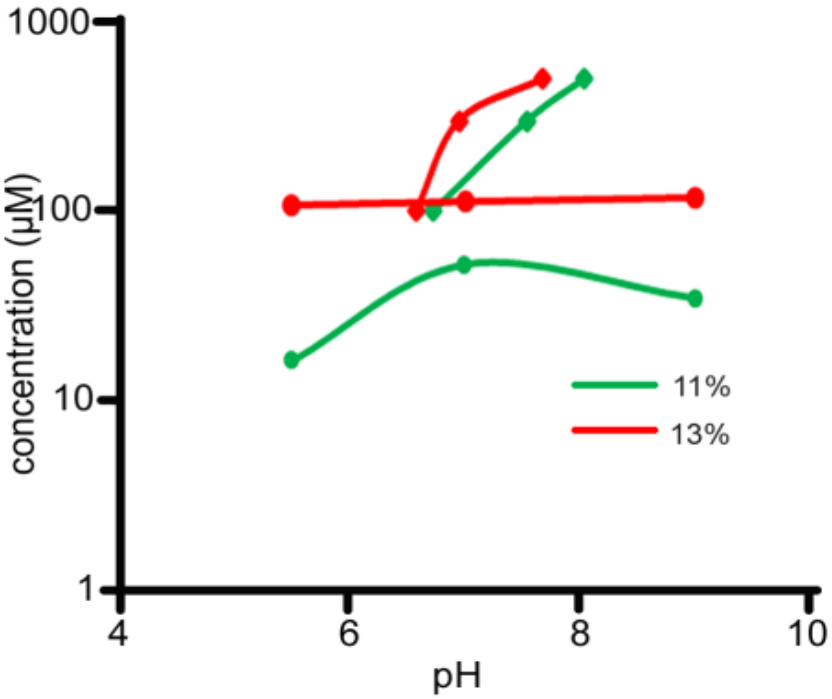

Figure 15: Phase diagram complied from CD and CAC data of varying concentrations of PA3PEG in relation to PA2 in artificial serum.

Chapter 4: Conclusion and Future Work

The characterization of the effects of PEGylation has revealed that its incorporation can affect self assembly. CD analysis found that an increase in PA3PEG concentration disrupts self assembly. More PA3PEG disrupts the ability of the micelle to transform into a nanofiber. Understanding how PEG changes assembly behavior is important because the vehicles that deliver the MRI contrast agent need to be fine-tuned to transition upon the slightly lower pH (6.4-7.2) of the microenvironment of the cancer cells compared to that of the blood pH (7.4).

The CAC studies found that an increase in PA3PEG concentration disrupts self assembly. A higher percentage of PA3PEG at a given pH increases the concentration of PA needed to allow for self-assembly into micelles or nanofibers. Understanding how PEG incorporation affects the transitioning concentration is important because the nanovehicle has to aggregate at concentration that is at least the concentration of Gd3+ needed to effectively image with MRI (10 μM).

A comparison of the phase diagrams of $C_{16}VA_3E_4$KDO3A:Gd and $C_{16}IA_3E_4$KDO3A:Gd both with PA3PEG gives information about how β -sheet propensity affects the amount of PA3PEG needed for a transition near pH 7. PAs that have greater propensity to form nanofibers, for example C_{16}-IA_3E_4KDO3A:Gd, need more relative amounts of PEGylated PA's to maintain a transition at a uniform pH.

CMC, CD, and TEM data offers information about how PEG incorporation affects the self assembly behavior of the synthesized PAs. Future research will also entail performing mouse experiments to confirm the biocompatibility of the PAs. Experiments in true serum are a necessary step to come closer to having the PA system become FDA

approvable. This research will find how the PAs accumulate in the body and how long they circulate before being targeted by phagocytes or by being eliminated by the body.

References

1. "Cancer Facts & Figures 2017" American Cancer Society. Web. 2017
2. Smith, R. A.; Cokkinides, V.; Eyre, H. J. American Cancer Society guidelines for the early detection of cancer, 2003. *Ca-a Cancer Journal for Clinicians* 2003, *53*, 27.
3. Cancer of the Breast Surveillance Epidemiology and End Results. Web. 2011. *Surveillance Epidemiology and End Results, Web*.
4. Barrett T., Brechbiel M., Bernardo M., Choyke P.L. MRI of tumor angiogenesis. Journal of Magnetic Resonance Imaging. 2007; 26:235-49
5. Islam T., Josephson L. Current state and future applications of active targeting in malignancies using superparamagnetic iron oxide nanoparticles. Cancer Biomarkers. 2009; 5:99-107
6. Bull, S.R.; Gula, M.O.; Bras, R.E.; Meade, T.J.; Stupp, S.I. "Self-Assembled Peptide Amphiphile Nanofibers Conjugated to MRI Contrast Agents," Nano Lett., 2005, 5, 1
7. Stubbs, M.; McSheehy, P. M. J.; Griffiths, J. R.; Bashford, C. L. Causes and consequences of tumour acidity and implications for treatment. *Molecular Medicine Today* 2000, *6*, 15.
8. Hashim, A. I.; Zhang, X.; Wojtkowiak, J. W.; Martinez, G. V.; Gillies, R. J. Imaging pH and metastasis. *Nmr in Biomedicine* 2011, *24*, 582.
9. Maeda, H.; Wu, J.; Sawa, T.; Matsumura, Y.; Hori, K. Tumor vascular permeability and the EPR effect in macromolecular therapeutics: a review. *Journal of Controlled Release* 2000, *65*, 271.
10. Maeda, H. Tumor-Selective Delivery of Macromolecular Drugs via the EPR Effect: Background and Future Prospects. *Bioconjugate Chemistry* 2010, *21*, 797.
11. Maeda, H. In *Advances in Enzyme Regulation, Vol 41*; Weber, G., Ed. 2001; Vol. 41, p 189.
12. Ghosh, A. et al; *JACS*, **2012**, 134 (8), 3647-50
13. Cui, H.; Webber, M. J.; Stupp, S. I. Self-Assembly of Peptide Amphiphiles: From Molecules to Nanostructures to Biomaterials. *Biopolymers* 2010, *94*, 1.
14. Webber, M. J.; Berns, E. J.; Stupp, S. I. Supramolecular Nanofibers of Peptide Amphiphiles for Medicine. *Israel Journal of Chemistry* 2013, *53*, 530.174
15. Meng, Q.; Kou, Y.; Ma, X.; Guo, L.; Liu, K. Nanostructures from the self- assembly of alpha-helical peptide amphiphiles. *Journal of Peptide Science* 2014, *20*, 223.
16. Missirlis, D.; Chworos, A.; Fu, C. J.; Khant, H. A.; Krogstad, D. V.; Tirrell, M. Effect of the Peptide Secondary Structure on the Peptide Amphiphile Supramolecular Structure and Interactions. *Langmuir* 2011, *27*, 6163.
17. Pashuck, E. T.; Cui, H.; Stupp, S. I. Tuning Supramolecular Rigidity of Peptide Fibers through Molecular Structure. *Journal of the American Chemical Society* 2010, *132*, 6041.
18. Manos, Aaron A. Thesis. The Ohio State University, **2016**.
19. Luan, J.; Yang, X.; Chu, L.; Xi, Y.; Zhai, G. PEGylated long circulating nanostructured lipid carriers for Amoitone B: Preparation, cytotoxicity and intracellular uptake. *Journal of colloid and interface science* 2014, *428*, 49.
20. Li, S.-D.; Huang, L. Pharmacokinetics and biodistribution of nanoparticles. *Molecular Pharmaceutics* 2008, *5*, 496.
21. Kim, C. W. A.; Berg, J. M. Thermodynamic beta-sheet propensities measured using a zinc-finger host peptide. *Nature* 1993, *362*, 267.

22. Ghosh, A., et al; *JACS*, **2014**. 15 4488-4494
23. Ghosh, A., et al; *Langmir*, **2014**. 30 15383-15387